

HANSER

Sample Pages

Chan I. Chung

Extrusion of Polymers

Theory & Practice

ISBN: 978-3-446-42409-8

For further information and order see

<http://www.hanser.de/978-3-446-42409-8>
or contact your bookseller.

isothermal spinning of a Newtonian fluid and predicted the critical draw ratio of 20.210. Below the critical draw ratio, any disturbance along the filament is dampened out and the filament is stable. Above the critical draw ratio, any disturbance propagates along the filament as a wave, causing draw resonance. This prediction was supported by an experiment by Donnelly and Weinberger [62], using a Newtonian silicone oil. Hyun [63], using a kinematic wave theory for the throughput rate, predicted the critical draw ratio of 19.744 for isothermal Newtonian fluids. Mathematical analyses were extended to isothermal and non-isothermal power-law fluids [64, 65]. While some investigators suggested that the elasticity of a polymer melt would increase the critical draw ratio, Han and Kim [66] found in their experiment that the residual elastic stress reduced the critical draw ratio.

3.5.7 Flow Through Simple Dies

Analytical solutions of polymer melt flow can be obtained only for isothermal, steady flow through very simple dies. Transient flow cannot be analyzed because of the time dependence of viscosity. Analytical solutions for complex dies cannot be obtained because of the shear and time dependence of viscosity. However, computer programs based on finite element methods for complex dies are commercially available.

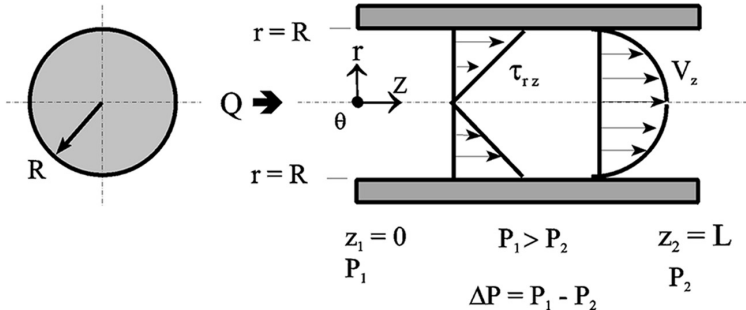
Analytical solutions for isothermal, steady flow through a circular tube and a slit (i.e., a wide flat opening without the ends) are presented below. These solutions have broad applications because the flow path in a small segment of many extrusion dies and adaptors can be approximated by a circular tube or a slit for the purpose of calculating pressure drop and flow rate. Dies for cast film and sheet are slits neglecting the two ends. Annular dies for blown film and blow molding are slits neglecting the curvature. A rectangular cross-section may be approximated by a circle. Although calculations based on such approximations will not give accurate predictions, the calculated values can serve as rough estimates.

3.5.7.1 Circular Tube

The isothermal, steady flow through a circular tube (or capillary) is analyzed in Section 3.5.3.1. Table 3.4 summarizes the analytical equations for isothermal, steady flow of Newtonian fluids and power-law fluids through a circular tube.

Table 3.4 Isothermal Flow Through Circular Tube

	Newtonian Fluid	Power-Law-Fluid
Viscosity	$\tau_w = \frac{\Delta P \cdot R}{2L}$	$\eta = \eta^0 \cdot \left(\frac{\dot{\gamma}}{\dot{\gamma}^0} \right)^{(n-1)}$ with $\dot{\gamma}^0 = 1.0 \text{ s}^{-1}$
Shear stress at the wall	$\tau_w = \frac{\Delta P \cdot R}{2L}$	$\tau_w = \frac{\Delta P \cdot R}{2L}$
Shear rate at the wall	$\dot{\gamma}_a = \frac{4Q}{\pi R^3}$	$\dot{\gamma}_w = \frac{\dot{\gamma}_a}{4} \cdot \left(3 + \frac{1}{n} \right)$
Maximum velocity at the tube center	$V_o = \frac{R^2 \cdot \Delta P}{4\mu L}$	$V_o = \left(\frac{R \cdot n \cdot \dot{\gamma}^0}{n + 1} \right) \cdot \left(\frac{R \cdot \Delta P}{2\eta^0 \cdot \dot{\gamma}^0 \cdot L} \right)^{1/n}$
Average velocity	$V_{\text{avg}} = \frac{1}{2} V_o$	$V_{\text{avg}} = \left(\frac{n + 1}{3n + 1} \right) \cdot V_o$
Volumetric flow rate	$Q = \frac{\pi R^4 \cdot \Delta P}{8\mu L}$	$Q = \pi R^2 \cdot V_{\text{avg}}$
Pressure drop	$\Delta P = \frac{8\mu L \cdot Q}{\pi R^4}$	$\Delta P = \left[\frac{Q}{\pi R^3} \cdot \left(\frac{3n + 1}{n \cdot \dot{\gamma}^0} \right) \right]^n \cdot \left(\frac{2\eta^0 \cdot \dot{\gamma}^0 \cdot L}{R} \right)$
Velocity profile	$V_z(r) = V_o \cdot \left[1 - \left(\frac{r}{R} \right)^2 \right]$	$V_z(r) = V_o \cdot \left[1 - \left(\frac{r}{R} \right)^{(n+1)/n} \right]$
Shear rate profile	$\dot{\gamma}(r) = \left(\frac{2V_o}{R} \right) \cdot \left(\frac{r}{R} \right)$	$\dot{\gamma}(r) = \left(\frac{V_o}{R} \right) \cdot \left(\frac{n+1}{n} \right) \cdot \left(\frac{r}{R} \right)^{1/n}$



3.5.7.2 *Slit*

Table 3.5 summarizes the analytical equations for isothermal, steady flow of Newtonian fluids and power-law fluids through a slit.

Example 3.9 Pressure Drop Through a Circular Die

A high density polyethylene (HDPE) with 0.950 g/cm^3 density, used in Example 3.5, is extruded through a circular die with 10 mm diameter and 100 mm length at the melt temperature of $190 \text{ }^\circ\text{C}$ to produce a rod. The viscosity data of the HDPE at $190 \text{ }^\circ\text{C}$ are given in the figure of Example 3.5 in Section 3.5.2.2. The density of HDPE at $190 \text{ }^\circ\text{C}$ is 0.7612 g/cm^3 .

Calculate the pressure drop through the die and the shear rate at the die wall for the two production rates given below.

1. Production rate = 100 kg/h
2. Production rate = 200 kg/h

Discuss factors that might affect the accuracy of the calculated results.

Solution:

The equations in Table 3.4 for the flow through a circular tube are used in the following calculations.

1. Production rate = 100 kg/h

The flow rate is

$$Q = 100,000 \frac{\text{g}}{\text{h}} \times \frac{1 \text{ h}}{3,600 \text{ s}} \times \frac{1 \text{ cm}^3}{0.7612 \text{ g}} = 36.49 \text{ cm}^3/\text{s}$$

Newtonian fluid method:

The apparent shear rate at the die wall is

$$\dot{\gamma}_a = \frac{4Q}{\pi R^3} = \frac{4 \times 36.49 \text{ cm}^3/\text{s}}{3.14 \times (0.5 \text{ cm})^3} = 371.9 \text{ s}^{-1}$$

The viscosity at 371.9 s^{-1} is read from the figure in Example 3.5.

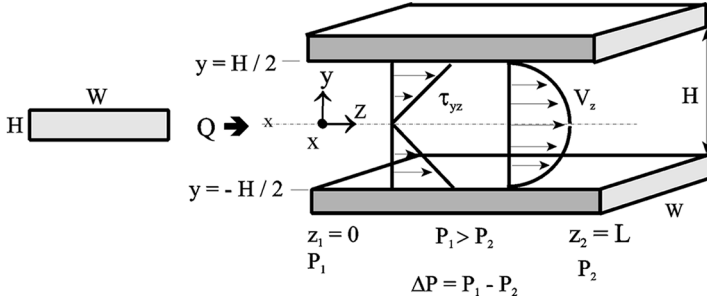
$$\eta = \mu \approx 400 \text{ Pa}\cdot\text{s}$$

The pressure drop according to the Newtonian fluid equation is

$$\Delta P = \frac{8\mu L \cdot Q}{\pi R^4} = \frac{8 \times 400 \text{ Pa}\cdot\text{s} \times 10 \text{ cm} \times 36.49 \text{ cm}^3/\text{s}}{3.14 \times (0.5 \text{ cm})^4} = 5,950 \text{ kPa (862 psi)}$$

Table 3.5 Isothermal Flow Through Slit

	Newtonian Fluid	Power-Law-Fluid
Viscosity	$\eta = \mu = \text{constant}$	$\eta = \eta^0 \cdot \left(\frac{\dot{\gamma}}{\dot{\gamma}^0} \right)^{(n-1)}$ with $\dot{\gamma}^0 = 1.0 \text{ s}^{-1}$
Shear stress at the wall	$\tau_w = \frac{\Delta P \cdot H}{2L}$	$\tau_w = \frac{\Delta P \cdot H}{2L}$
Shear rate at the wall	$\dot{\gamma}_a = \frac{6Q}{W \cdot H^2}$	$\dot{\gamma}_w = \frac{\dot{\gamma}_a}{3} \cdot \left(\frac{2n+1}{n} \right)$
Maximum velocity at the mid-plane	$V_o = \frac{H^2 \cdot \Delta P}{8\mu L}$	$V_o = \frac{H}{2} \left(\frac{n \cdot \dot{\gamma}^0}{n+1} \right) \cdot \left(\frac{H \cdot \Delta P}{2\eta^0 \cdot \dot{\gamma}^0 \cdot L} \right)^{1/n}$
Average velocity	$V_{\text{avg}} = \frac{2}{3} V_o$	$V_{\text{avg}} = \left(\frac{n+1}{2n+1} \right) \cdot V_o$
Volumetric flow rate	$Q = \frac{W \cdot H^3 \cdot \Delta P}{12\mu L}$	$Q = W \cdot H \cdot V_{\text{avg}}$
Pressure drop	$\Delta P = \frac{12\mu L \cdot Q}{W \cdot H^3}$	$\Delta P = \left[\left(\frac{2Q}{W \cdot H^2} \right) \cdot \left(\frac{2n+1}{n \cdot \dot{\gamma}^0} \right) \right]^n \cdot \left(\frac{2\eta^0 \cdot \dot{\gamma}^0 \cdot L}{H} \right)$
Velocity profile	$V_z(y) = V_o \cdot \left[1 - \left \frac{2y}{H} \right ^2 \right]$	$V_z(y) = V_o \cdot \left[1 - \left \frac{2y}{H} \right ^{(n+1)/n} \right]$
Shear rate profile	$\dot{\gamma}(y) = \left(\frac{4V_o}{H} \right) \cdot \left \frac{2y}{H} \right $	$\dot{\gamma}(y) = \left(\frac{2V_o}{H} \right) \cdot \left(\frac{n+1}{n} \right) \cdot \left \frac{2y}{H} \right ^{1/n}$



Power-law fluid method:

The shear rate in the die is maximum at the die wall and decreases toward the center of the die, becoming zero at the center. The important shear rate in this calculation is the true shear rate at the die wall, which will be higher than the apparent shear rate of 371.9 s^{-1} . Calculation of the true shear rate requires the power-law exponent, n , whose value depends on the range of shear rate. Referring to Example 3.5 in Section 3.5.2.2, the power-law for the HDPE covering the shear rate range of about $30\text{--}300 \text{ s}^{-1}$ was found to be

$$\eta = \eta^0 \cdot \dot{\gamma}^{(n-1)}, \quad \text{where } \eta^0 = 17,589 \text{ Pa}\cdot\text{s} \text{ and } n = 0.378$$

The above power-law constants will be assumed to be applicable to the true shear rate at the die wall. The true shear rate at the die wall is

$$\dot{\gamma}_w = \frac{\dot{\gamma}_a}{4} \cdot \left(3 + \frac{1}{n} \right) = \frac{371.9 \text{ s}^{-1}}{4} \times \left(3 + \frac{1}{0.378} \right) = 524.9 \text{ s}^{-1}$$

The true shear rate is found to be 1.41 times the apparent shear rate because of the high shear sensitivity of the viscosity with a small value of n . The power-law viscosity at 524.9 s^{-1} is

$$\eta = \eta^0 \cdot \dot{\gamma}^{(n-1)} = 17,589 \text{ Pa}\cdot\text{s} \times (598.3)^{(0.378-1)} = 329.8 \text{ Pa}\cdot\text{s}$$

The pressure drop according to the power-law fluid equation is

$$\begin{aligned} Q &= \pi R^2 \cdot V_{\text{avg}} = \pi R^2 \cdot \left(\frac{n+1}{3n+1} \right) \cdot V_0 \\ &= \pi R^2 \cdot \left(\frac{n+1}{3n+1} \right) \cdot \left(\frac{nR \cdot \dot{\gamma}^0}{n+1} \right) \cdot \left(\frac{R \cdot \Delta P}{2\eta^0 \cdot \dot{\gamma}^0 \cdot L} \right)^{1/n} \\ \Delta P &= \left[\frac{Q}{\pi R^3} \cdot \left(\frac{3n+1}{n \cdot \dot{\gamma}^0} \right) \right]^n \cdot \left(\frac{2\eta^0 \cdot \dot{\gamma}^0 \cdot L}{R} \right) \\ &= \left[\frac{36.49 \text{ cm}^3/\text{s}}{3.14 \times (0.5 \text{ cm})^3} \cdot \left(\frac{3 \times 0.378 + 1}{0.378 \times 1.0 \text{ /s}} \right) \right]^{0.378} \\ &\quad \cdot \left(\frac{2 \times 17,589 \text{ Pa}\cdot\text{s} \times 1.0/\text{s} \times 10 \text{ cm}}{0.5 \text{ cm}} \right) = 7,507 \text{ kPa (1,088 psi)} \end{aligned}$$

2. Production rate = 200 kg/h

The calculations performed above for the production rate of 100 kg/h are repeated.

The flow rate is

$$Q = 200,000 \frac{\text{g}}{\text{h}} \times \frac{1 \text{ h}}{3,600 \text{ s}} \times \frac{1 \text{ cm}^3}{0.7612 \text{ g}} = 72.98 \text{ cm}^3/\text{s}$$

Newtonian fluid method:

The apparent shear rate at the die wall is

$$\dot{\gamma}_a = \frac{4Q}{\pi R^3} = \frac{4 \times 72.98 \text{ cm}^3/\text{s}}{3.14 \times (0.5 \text{ cm})^3} = 743.8 \text{ s}^{-1}$$

The viscosity at 743.8 s^{-1} is read from the figure in Example 3.5, and it is

$$\eta = \mu \approx 240 \text{ Pa}\cdot\text{s}$$

The pressure drop according to the Newtonian fluid equation is

$$\Delta P = \frac{8\mu L \cdot Q}{\pi R^4} = \frac{8 \times 240 \text{ Pa}\cdot\text{s} \times 10 \text{ cm} \times 72.98 \text{ cm}^3/\text{s}}{3.14 \times (0.5 \text{ cm})^4} = 7,140 \text{ kPa (1,034 psi)}$$

Power-law fluid method:

The apparent shear rate at the die wall is 743.8 s^{-1} in this case, and the true shear rate at the die wall will be even higher. Referring to the figure in Example 3.5, the power-law equation covering the shear rates below about 300 s^{-1} used in the previous case for 100 kg/h rate will substantially overestimate the viscosity around 800 s^{-1} . It is noted that a small difference on logarithmic scale is actually a large difference in numbers. The power-law equation for shear rates over 150 s^{-1} in Example 3.5 is a better choice in this case.

$$\eta = \eta^0 \cdot \dot{\gamma}^{(n-1)} \quad \text{where } \eta^0 = 51,425 \text{ Pa}\cdot\text{s} \text{ and } n = 0.184$$

The true shear rate at the die wall is

$$\dot{\gamma}_w = \frac{\dot{\gamma}_a}{4} \cdot \left(3 + \frac{1}{n} \right) = \frac{743.8 \text{ s}^{-1}}{4} \times \left(3 + \frac{1}{0.184} \right) = 1,568.4 \text{ s}^{-1}$$

The true shear rate is found to be more than twice the apparent shear rate in this case because of the very small value of n . The power-law viscosity at $1,568.4 \text{ s}^{-1}$ is

$$\eta = \eta^0 \cdot \dot{\gamma}^{(n-1)} = 51,425 \text{ Pa}\cdot\text{s} \times (1,568.4)^{(0.184-1)} = 127 \text{ Pa}\cdot\text{s}$$

The pressure drop according to the power-law fluid equation is

$$\begin{aligned} \Delta P &= \left[\frac{Q}{\pi R^3} \cdot \left(\frac{3n+1}{n \cdot \dot{\gamma}^0} \right) \right]^n \cdot \left(\frac{2\eta^0 \cdot \dot{\gamma}^0 \cdot L}{R} \right) \\ &= \left[\frac{72.98 \text{ cm}^3/\text{s}}{3.14 \times (0.5 \text{ cm})^3} \cdot \left(\frac{3 \times 0.184 + 1}{0.184 \times 1.0 / \text{s}} \right) \right]^{0.184} \\ &\quad \cdot \left(\frac{2 \times 51,425 \text{ Pa}\cdot\text{s} \times 1.0 / \text{s} \times 10 \text{ cm}}{0.5 \text{ cm}} \right) \\ &= 7,965 \text{ kPa} (1,154 \text{ psi}) \end{aligned}$$

The results of the above calculations are summarized below.

Output rate	100 kg/h	200 kg/h
Pressure drop, kPa (psi)		
Newtonian fluid method	5,950 (862)	7,140 (1,034)
Power-law fluid method	7,507 (1,088)	7,965 (1,154)
Shear rate at the die wall, s^{-1}		
Newtonian fluid method	371.9	743.8
Power-law fluid method	524.9	1,568.4

The Newtonian fluid method estimates the pressure drop through the die significantly lower than the power-law fluid method. The pressure drop through the die does not increase proportional to the output rate because of the shear thinning effect of the viscosity. When the output rate is increased by 100%, the pressure drop is found to increase by about 20%, according to the Newtonian fluid method, or only about 6%, according to the power-law fluid method. The true shear rate at the die wall is greatly higher than the apparent shear rate at the die wall because of the low value of n .

The factors affecting the accuracy of the above calculations include the following:

(a) The Newtonian fluid method is obviously incorrect because the viscosity of the HDPE melt is highly pseudoplastic. The power-law fluid method should give better predictions. However, the predictions of the power-law fluid method depend on the values of n and η° . Because the values of n and η° depend on shear rate range and they are not exact, the predictions are not exact.

(b) An isothermal condition was assumed, neglecting any melt temperature variation and heat generation within the melt. Heat generation on the die wall will be significant, reducing the viscosity, especially for a long die, and the actual pressure drop will be lower than the predicted value.

(c) The melt flows from an adaptor with a large cross-section into the small circular die, and the flow is not at a steady-state near the entrance of the die. The calculations were made using the steady flow viscosity. The shear rate inside the adaptor will be lower than that inside the die, and the viscosity inside the adaptor will be higher than that inside the die. The viscosity will decrease from the value inside the adaptor to the value inside the die, taking a finite time. The actual pressure drop will be slightly higher than the predicted value, but this effect will not be as significant as the effect of heat generation.

Example 3.10 Pressure Drop Through a Blown Film Die

A blown film line runs a linear low density polyethylene (LLDPE) with $[MI] = 1.0$ and 0.910 g/cm^3 density. The annular die lip has 25.4 cm (10 in) diameter, 0.254 cm (0.1 in) gap opening and 5.08 cm (2.0 in) land length. The desired output rate is 142.4 kg/h (314 lbs/h) or 1.7858 kg/h per one cm of the die circumference (10 lbs/h per one inch of the die circumference) at 250 °C (482 °F) melt temperature. The melt viscosity and the melt density of the polymer at 250 °C (482 °F) are given by

$$\eta = \eta^\circ \cdot \dot{\gamma}^{(n-1)} \quad \text{where } \eta^\circ = 4,375 \text{ Pa}\cdot\text{s} \text{ (0.634 lb}_f\text{-s/in}^2\text{)} \text{ and } n = 0.654$$

$$\rho_m = 0.7303 \text{ g/cm}^3$$

Calculate the shear rate at the die wall and the pressure drop through the die lip.

Solution:

The annular die lip can be treated as a slit by unwrapping it and placing it on a flat surface. The dimensions of the equivalent slit are

$$W = \pi D = 3.14 \times 25.4 \text{ cm} = 79.756 \text{ cm}$$

$$H = 0.254 \text{ cm}$$

$$L = 5.08 \text{ cm}$$

The power-law fluid equations for isothermal flow through a slit in Table 3.5 will be used in the following calculations.

The flow rate is

$$Q = 142,400 \frac{\text{g}}{\text{h}} \times \frac{1 \text{ h}}{3,600 \text{ s}} \times \frac{1 \text{ cm}^3}{0.7303 \text{ g}} = 54.1634 \text{ cm}^3/\text{s}$$

The true shear rate at the die wall is

$$\begin{aligned} \dot{\gamma}_w &= \frac{\dot{\gamma}_a}{2} \cdot \left(\frac{n+1}{n} \right) = \left(\frac{6Q}{W \cdot H^2} \right) \times \frac{1}{2} \times \left(\frac{n+1}{n} \right) \\ &= \left(\frac{6 \times 54.1634 \text{ cm}^3/\text{s}}{79.756 \text{ cm} \times (0.254 \text{ cm})^2} \right) \times \frac{1}{2} \times \left(\frac{0.654 + 1}{0.654} \right) = 79.86 \text{ s}^{-1} \end{aligned}$$

The pressure drop is

$$\begin{aligned} \Delta P &= \left[\left(\frac{2Q}{W \cdot H^2} \right) \cdot \left(\frac{2n+1}{n \cdot \dot{\gamma}^o} \right) \right]^n \cdot \left(\frac{2\eta^o \cdot \dot{\gamma} \cdot L}{H} \right) \\ &= \left[\left(\frac{2 \times 54.1634 \text{ cm}^3/\text{s}}{79.756 \text{ cm} \times (0.254 \text{ cm})^2} \right) \cdot \left(\frac{2 \times 0.654 + 1}{0.654 \times 1.0 / \text{s}} \right) \right]^{0.654} \\ &\quad \cdot \left(\frac{2 \times 4,375 \text{ Pa} \cdot \text{s} \times 1.0 / \text{s} \times 5.08 \text{ cm}}{0.254} \right) \\ &= 2,928.6 \text{ kPa (424.4 psi)} \end{aligned}$$

3.5.8 Elastic Memory Effect on Extrudate Shape

A polymer melt is viscoelastic with a characteristic relaxation time (see Section 3.5.1.1), and it has a memory of the stress/strain condition during a time period longer than the relaxation time after a stress/strain condition was applied. The relaxation time for a highly viscous and highly elastic polymer melt, such as high molecular weight-high density polyethylene (HMW-HDPE) and rigid polyvinyl chloride, can be very long, on the order of minutes.

The shape and layer structure, if coextruded, of an extrudate exiting a die are influenced by the previous stress/strain history leading to the die exit, and they may be quite different

5 Screw Design, High Performance Screws, and Scale-Up

5.1 Screw Design

5.1.1 General Screw Design Guidelines

The screw is the only working component of an extruder. The performance of the extruder, such as the output rate, melt temperature, melt quality and stability, depends primarily on the screw design. The following design parameters are decided in the screw design, in logical order:

- Screw diameter and length
- Screw material, and special surface treatment if necessary
- Cooling bore and its length if necessary
- Single-stage or multiple-stages
- Number of parallel flights
- Pitch (or lead)
- Flight width and radii on the screw root
- Wear resistance of the flight land
 - Chemical treatment, flame-hardening or welding of a special hard alloy
- Metering section depth and length
- Compression section length (or taper)
- Feeding section depth and length
- Mixing section or head
- Special channel geometry

The output rate per rpm, called the “specific output rate”, mainly depends on the metering depth. A deeper metering section usually gives a higher specific output rate and a lower melt temperature, but an inferior melt quality. Because the melt temperature is the most important operating parameter in extrusion, the metering depth is the most important design parameter. The optimum metering depth depends on the viscosity of the polymer, the head pressure, and the desired melt temperature in the process. Because a polymer with higher viscosity generates more heat, resulting in higher melt temperature, it requires a deeper metering

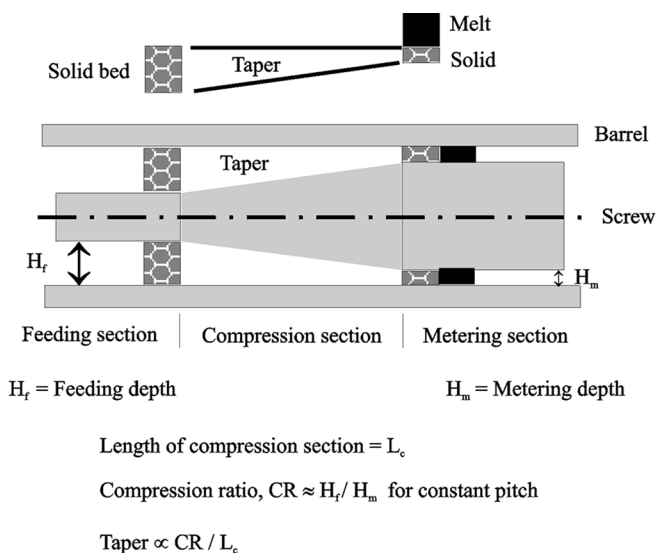


Figure 5.1 Taper in compression section and reduction rate of solid bed thickness

section to avoid undesirably high melt temperatures. The specific output rate of a screw with a deeper metering section decreases faster with increasing head pressure (see Chapter 4; Fig. 4.43), and the optimum metering depth is shallower at higher head pressure (see Chapter 4; Fig. 4.44). The optimum metering depth for a given polymer also depends on the process. A blown film process requires a lower melt temperature than a cast film process, and thereby a deeper metering section. Blow molding requires a low melt temperature for good melt strength, and thereby a deep metering section. Furthermore, the optimum metering depth for a given polymer in a given process depends on the desired melt quality for the particular product. A better melt quality requires a shallower metering section.

The compression ratio (CR) of a screw is approximated by the ratio of the feeding depth to the metering depth for screws with a constant pitch. The CR is a very important design parameter, but the CR by itself is not a sufficient design parameter. The taper of the screw channel in the compression section shown in Fig. 5.1 should be the design parameter instead of the CR. For screws with a constant pitch, the taper of the screw channel is set by both the CR and the length of the compression section. For a given CR, a longer compression section gives a lesser taper. The solid bed thickness is reduced as it melts along the compression section. The taper in the compression section should be less than, or preferably equal to, the reduction rate of the solid bed thickness along the compression section. If the taper is more than the reduction rate of the solid bed thickness, the tightly packed solid bed will be wedged in the screw channel until it melts sufficiently to pass through the screw channel. Such wedging of the solid bed is a frequent cause of surging. If the taper is less than the reduction rate of the solid bed thickness, the solid bed will not be pressed on the barrel surface and the dissipative melting rate Ω of the solid bed on the barrel surface will be decreased. A polymer

with a higher Ω gives a faster reduction rate of the solid bed thickness and requires a greater taper with a shorter compression section at a given CR, whereas a polymer with a lower Ω requires a lesser taper with a longer compression section at a given CR.

Polymers with a high viscosity (or a high friction coefficient) develop a high pressure in the feeding section and give a high solid conveying rate. A reasonable pressure level at the end of the feeding section is necessary for pressure stability, but an undesirably high pressure increases the melt temperature and the screw wear. A low CR of about 2–2.5 is used for polymers with a high viscosity, while a high CR of about 3–5 is used for polymers with a low viscosity. Rigid polymers, which are hard to compress, need a high CR to develop a high pressure.

The production rate of a single-screw extruder is often limited by the melting capacity of the screw. An extruder used only as a solid conveyor or a melt pump for a polymer has an output rate many times greater than the same size extruder used to melt the polymer. The melting capacity of a screw comes mostly from the dissipative melting of the solid bed rubbing on the barrel. Both the area of the solid bed in contact with the barrel and the dissipative melting rate of the solid bed must be maximized to achieve the maximum output rate. Special screw geometries can be utilized to maximize the solid bed area or the melting rate. The melting rate decreases with increasing solid bed width (see Chapter 4; Section 4.3.1). Because the solid bed width is proportional to the channel width, the channel width is an important design parameter, especially for large screws in scale-up. Use of multiple flights for large diameter screws reduces the channel width and increases the melting rate, but reduces the melting area and increases the power consumption because of increased flight area.

5.1.2 Scientific Screw Design Method

Screw design technology has been largely empirical and secretive. However, it is possible to design a screw scientifically by utilizing the advances made in the extrusion technology [1, 2].

Predictions of the melting rate Ω of the solid bed and the melting capacity G_m of a screw, presented in Chapter 4; Section 4.3.1, are the most important tasks in designing the screw scientifically. Once the melting rate and the melting capacity are predicted, the metering section, the compression section, and the feeding section can be designed scientifically as described by the following steps:

Step 1: Calculate (or measure) the melting rate of the solid bed at the expected operating screw speed and barrel temperature.

Step 2: Estimate the melting capacity of the screw using the melting rate of the solid bed and the maximum possible solid bed area. If the estimated melting capacity is less than the desired output rate, increase the expected operating screw speed and repeat Steps 1 and 2 until the estimated melting capacity becomes at least equal to the desired output rate. The output rate cannot be more than the estimated melting capacity.

Step 3: Determine the optimum depth and length of the metering section to match the metering rate, that is, the output rate, with the melting capacity against the expected head pressure, and also to achieve the desired output rate stability with a probable fluctuation in the head pressure of about $\pm 1.0\%$.

Step 4: Determine the optimum feeding depth and compression section length to match the taper of the compression section with the reduction rate of the solid bed thickness and to assure complete melting of the solid bed in the metering section.

Step 5: Adjust the calculated design parameters, considering common practice and other relevant factors.

Example 5.1 illustrates the above screw design method in detail.

Example 5.1 Scientific Screw Design Method

Design a 152.4 mm (6 in) D, $L/D = 32$, screw to run a branched low density polyethylene (BLDPE) with 0.92 g/cc density in a blown film operation. The polymer is the same one used in Chapter 4; Example 4.6. The desired output rate is 1,045 kg/h (2,300 lbs/h) at a melt temperature below 230 °C (446 °F) against 27.6 MPa (4,000 psi) head pressure. The screw will have a single flight with square-pitch and a single-stage. The axial flight width will be 10% of the diameter.

The following polymer properties, repeated from Example 4.6, are necessary in the calculations.

The melt viscosity of the BLDPE as a function of shear rate and temperature;

$$\ln \eta^*(T, \dot{\gamma}) = C_0 + C_1 \cdot (\ln \dot{\gamma}) + C_2 \cdot (\ln \dot{\gamma})^2 + C_3 \cdot T \cdot (\ln \dot{\gamma}) + C_4 \cdot T + C_5 \cdot T^2$$

where η^* is in Pa-s, T in °C, and $\dot{\gamma}$ in s^{-1} .

The six constants for this sample are

$$\begin{array}{lll} C_0 = 11.739 & C_1 = -0.637 & C_2 = -8.367 \times 10^{-3} \\ C_3 = 7.218 \times 10^{-4} & C_4 = -0.014 & C_5 = 1.831 \times 10^{-6} \end{array}$$

The power-law equation at 230 °C (446 °F) over the shear rate range of about 10–300 s^{-1} in the metering channel is obtained from the above general equation with six constants

$$\eta = \eta^0 \cdot \dot{\gamma}^{(n-1)} \text{ with } \eta^0 = 7,080 \text{ Pa-s (1.026 lb}_f\text{-s/in}^2\text{) and } n = 0.448$$

Other relevant properties of the polymer are as follows:

$k_m = 5.5 \times 10^{-4}$ cal/cm-°C-s, thermal conductivity of the melt in the direction normal to the flow

$\rho_m = 0.863 - 5.324 \times 10^{-4} \cdot T$ g/cm³-°C with T in °C, melt density

$T_f = 117$ °C, flow temperature taken as the end of the melting range

$C_{pm} = 0.5916 \text{ cal/g}\cdot^\circ\text{C}$, specific heat capacity of the melt

$\Delta H = 82.8172 \text{ cal/g}$, enthalpy difference between the melt at the flow temperature T_f and the solid polymer at the feed temperature T_s

Solution:

The screw will be designed following the steps described in Section 5.1.2. The melting rate Ω and the shear stress τ of a solid bed depend on the solid bed width X_o . Because X_o changes along the screw, as shown in Chapter 4; Fig. 4.36, different values of Ω and τ will be calculated for different segments of the solid bed along the screw in an actual design process. However, a constant Ω and a constant τ will be used in this example for simplicity, assuming a constant average X_o along the screw. The differential pressure P_o between the solid bed and the melt pool is not known. However, the effects of P_o on Ω and τ are expected to be minimal, as illustrated in Chapter 4; Example 4.6, and the effects of P_o will be ignored.

The solid bed rubs on the barrel surface in the θ -direction at the velocity of U_{sb} , as described in Chapter 4; Section 4.2. Because the solid conveying angle θ is very small, in the range of $2\text{--}3^\circ$, it is safe to assume that the solid bed is attached on the screw and rotates with the screw for the purpose of this example.

$$U_{sb} \approx U_s = N\pi D$$

The screw channel is full of the solid bed at the start of melting and becomes full of the melt pool at the end of melting. The average solid bed width is assumed to be 50% of the channel width in the direction of the screw rotation around the screw circumference.

$$X_o = 0.5 \times \left(\pi D - \frac{F}{\tan \phi} \right) = 0.5 \times \left(3.14 \times 6 \text{ in} - \frac{0.1 \times 6 \text{ in}}{\tan 17.7^\circ} \right) \times 2.54 \text{ cm/in} = 21.54 \text{ cm}$$

Step 1: Calculation of Ω and τ of the solid bed

Three barrel temperatures and two operating screw speeds are considered.

Barrel temperature $T_b = 170, 190$ and 220°C , respectively

Screw speed $U_{sb} = 23.9 \text{ cm/s}$ at 30 rpm and 79.8 cm/s at 100 rpm

Ω and τ in each case are calculated following the same procedure as in Example 4.6.

$X_o = 21.54 \text{ cm}$ is used in all cases. The results are given in the following table.

The results shown in the table are quite interesting. With increasing T_b , Ω increases slightly at 30 rpm but decreases slightly at 100 rpm. τ decreases substantially with increasing T_b at both screw speeds. The effect of T_b on Ω is small as long as T_b is much higher than the flow temperature T_f . Ω decreases with increasing T_b if the decrease in heat generation in the melt film, caused by reduced viscosity, is more than the increase in heat conduction from the barrel. τ always decreases with increasing T_b because of reduced viscosity.

Case No.	rpm	T_b , °C	U_{sb} , cm/s	Ω , g/cm ² -s	τ , MPa
1	30	170	23.9	0.01752	0.270
2	30	190	23.9	0.01829	0.233
3	30	220	23.9	0.01897	0.188
4	100	170	79.8	0.04049	0.461
5	100	190	79.8	0.04049	0.411
6	100	220	79.8	0.03997	0.346

τ at 100 rpm is much higher than τ at 30 rpm. The motor power necessary for melting the solid bed is proportional to the screw rpm times τ .

Motor power \propto (rpm) \cdot τ

$$\frac{(\text{Motor power})_2}{(\text{Motor power})_1} = \left[\frac{(\text{rpm})_2}{(\text{rpm})_1} \right] \cdot \left(\frac{\tau_2}{\tau_1} \right)$$

The motor power necessary for melting the solid bed will increase more than proportional to screw rpm because τ_2 is higher than τ_1 . This is an important part of the reason why the motor power always increases more than proportional to screw rpm in all extrusion operations.

Note – The polymer properties required to calculate Ω and τ are not readily available for many polymers. Ω and τ can be measured experimentally using the screw simulator, shown in Chapter 4; Fig. 4.21. Because the solid bed width X_o in the screw simulator experiments is 2.54 cm (1.0 in) and it is much less than the actual solid bed width inside the screw in design, the measured Ω and τ must be corrected for the difference in the solid bed width. In the simplest case of temperature-independent viscosity analyzed in Case A of Chapter 4; Section 4.3.1.2.2.1, $\Omega \propto (1 / X_o^{1/2})$ and $\tau \propto (1 / X_o^{n/2})$.

Step 2: Estimation of the melting capacity of the screw

The melting capacity of the screw, G_m is the sum of the dissipative melting capacity of the solid bed and the conduction melting capacity. The conduction melting capacity is a minor fraction in comparison to the dissipative melting capacity and it will be ignored. Now, G_m is equal to Ω times the total solid bed area A_s along the screw.

$$G_m = \Omega \cdot A_s$$

The solid bed melts as soon as it contacts the hot barrel surface starting at about 3 (L/D) from the feed pocket of the screw, and it should completely melt at about 5 (L/D) before the end of the screw. Because the solid bed and the melt pool occupy the screw channel equally, on the average, the maximum total solid bed area is approximately 50% of the total barrel surface area less the portion occupied by the flight (10%), the first 3 (L/D), and the last 5 (L/D).

$$A_s = 0.5 \times 0.9 \times \pi \times (D^2) \times [(L/D) - 3 - 5]$$

$$= 0.5 \times 0.9 \times 3.14 \times (15.24^2) \times [32 - 3 - 5] = 7,876 \text{ cm}^2$$

The estimated melting capacities of the screw with $A_s = 7,876 \text{ cm}^2$ corresponding to the various cases in Step 1 are given below.

Case No.	rpm	T_b , °C	U_{sb} , cm/s	G_m , g/s (lbs/h)
1	30	170	23.9	138.0 (1,095)
2	30	190	23.9	144.1 (1,144)
3	30	220	23.9	149.4 (1,186)
4	100	170	79.8	318.9 (2,531)
5	100	190	79.8	318.9 (2,531)
6	100	220	79.8	314.8 (2,498)

The estimated melting capacity of the screw at 30 rpm is insufficient for the desired output rate of $290.7 \text{ g/s} = 1,045 \text{ kg/h}$ (2,300 lbs/h). The estimated melting capacity at 100 rpm is about 9% more than the desired output rate, and 100 rpm is selected as the expected operating screw speed.

Step 3: Determination of the optimum depth and length of the metering section

The metering or pumping rate of the metering section is the output rate G of the screw. The metering section must be able to pump G against the head pressure with the desired output rate stability. The output rate and the output rate instability are calculated as a function of the metering depth using the power-law fluid model presented in Chapter 4; Section 4.4.2. The same computer program used in Chapter 4; Example 4.8 is utilized for the duplicate calculations. The following input data are used in the computer calculations.

Melt density at 230 °C (446 °F), $\rho_m = 0.74 \text{ g/cm}^3$

Pitch, $P = 15.24 \text{ cm}$ (6 in)

Axial flight width, $F = 10\%$ of the diameter = 1.524 cm (0.6 in)

Metering depth, $H_m = 0.762 \text{ cm}$ (0.3 in) to 1.524 cm (0.6 in)

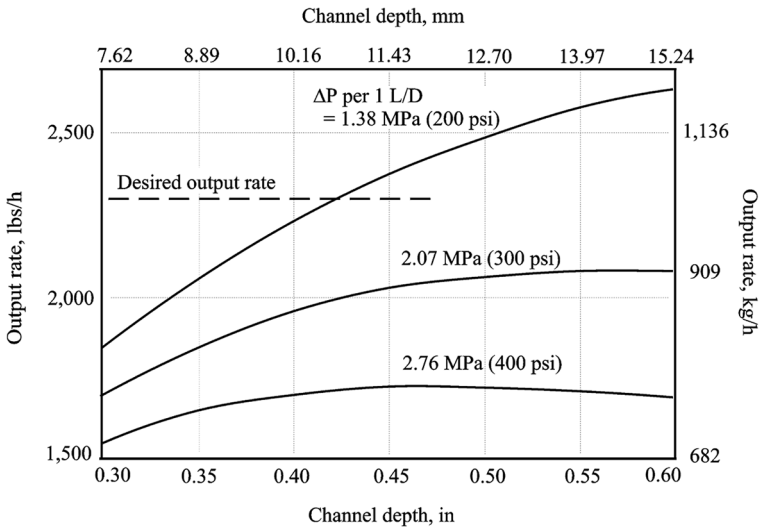
Pressure gradient, 1.38 MPa (200 psi), 2.07 MPa (300 psi) or 2.76 MPa (400 psi) per 1 L/D

Fluctuation of the pressure gradient = 0.069 MPa (10 psi) per 1 L/D, corresponding to 2.5% of the high pressure gradient of 2.76 MPa (400 psi) per 1 L/D.

Required output rate instability = less than 2% with the above fluctuation of the pressure gradient

The results are shown in the figure below.

152.4 mm (6 in) D. Metering section; 100 rpm
 Single flight with square-pitch and axial width = 10% of diameter
 Branched low density polyethylene, 0.92 g/cc, 0.85 [MI], at 230 °C



The desired output rate of 1,045 kg/h (2,300 lbs/h) can be obtained only at the low pressure gradient of 1.38 MPa per 1 L/D, and the metering depth H_m must be at least 1.067 cm. The desired output rate cannot be obtained at higher pressure gradients. The output rate decreases slightly with increasing H_m over about 1.143 cm at the high pressure gradient of 2.76 MPa per 1 L/D. Therefore, H_m should be less than about 1.143 cm. The output rate instability increases with increasing H_m . The predicted output rate and the output rate instability at the pressure gradient of 1.38 MPa per 1 L/D and 0.069 MPa pressure fluctuation per 1 L/D are given below at three values of H_m .

Metering Depth cm (in)	Output Rate kg/h (lbs/h)	Output Rate Instability, %
1.016 (0.40)	1,017 (2,237)	1.3
1.143 (0.45)	1,084 (2,385)	1.6
1.270 (0.50)	1,137 (2,502)	1.8

The output rate instability is less than 2% or $\pm 1\%$ at all metering depths, and the metering depth up to 1.27 cm (0.50 in) is acceptable as far as the output rate stability is concerned. Considering the desired output rate and output rate stability, the best metering depth is about 1.143 cm (0.45 in), and the maximum pressure gradient in the metering section is about 1.38 MPa (200 psi) per 1 L/D.

The required L/D ratio of the metering section is related to the maximum pressure gradient per 1 L/D by:

$$\text{L/D ratio of the metering section} = (P_h - P_i) / \text{Maximum pressure gradient per 1 L/D}$$

where

P_h = head pressure at the end of the screw

P_i = inlet pressure at the entrance of the metering section

The above relationship assumes that the pressure at the end of the metering section is equal to P_h . This assumption is correct unless a mixing head is placed after the metering section.

P_h is always measured for safety, but P_i is usually not measured. Three values of P_i will be assumed:

$$P_i = 6.9 \text{ MPa (1,000 psi)}$$

$$13.8 \text{ MPa (2,000 psi)}$$

$$20.7 \text{ MPa (3,000 psi)}$$

The required L/D ratio of the metering section for the three assumed values of P_i is calculated from the above relationship:

$$\text{For } P_i = 6.9 \text{ MPa, the required L/D ratio} = (27.6 \text{ MPa} - 6.9 \text{ MPa}) / 1.38 \text{ MPa} = 15$$

$$\text{For } P_i = 13.8 \text{ MPa, the required L/D ratio} = (27.6 \text{ MPa} - 13.8 \text{ MPa}) / 1.38 \text{ MPa} = 10$$

$$\text{For } P_i = 20.7 \text{ MPa, the required L/D ratio} = (27.6 \text{ MPa} - 20.7 \text{ MPa}) / 1.38 \text{ MPa} = 5$$

The very long, 15 L/D metering section required for $P_i = 6.9$ MPa (1,000 psi) does not leave enough screw length for other sections. Because it was assumed that melting was complete at 5 L/D before the end of the screw, the minimum metering length should be 5 L/D. Therefore, a 10 L/D metering section required for $P_i = 13.8$ MPa (2,000 psi) is